NOTES AND CORRESPONDENCE

Associations between North Atlantic Sea Surface Temperature Anomalies, Latitude of the Polar Front Zone, and Precipitation over Northwest Europe

A. MOENE

Norwegian Meteorological Institute, Oslo, Norway

1 December 1984 and 28 August 1985

ABSTRACT

Based on available data, a 100-year series of annual sea surface temperature (SST) is established for a given area in the North Atlantic. The oscillations of the annual SST anomalies are characterized as small oscillations about a stable state of equilibrium obviously determined by the heat balance.

The behavior of such a system can be described by linear integro-differential equations with constant coefficients. It is shown that the power spectrum of a second-order autoregressive linear stochastic process reveals the main features of the spectrum of the given SST time series. The observed low frequency significant peak of the annual SST anomaly spectrum is assumed to be the oceanic integral response to the white noise atmospheric input on shorter time scales. The low frequency location of the peak, corresponding to a period of 25–30 years, is physically explained by the large thermal inertia caused by the large heat capacity of the ocean.

A thermal feedback of low frequency SST oscillations to the atmosphere explains the low frequency latitudinal oscillations of the annual mean tropospheric thermal field, including the polar frontal zone from the North Atlantic toward Europe.

1. Introduction

As early as 1917, Helland-Hansen and Nansen found that the greatest sea surface temperature (SST) anomalies were produced by wind anomalies and appear and disappear over large sections of the North Atlantic almost simultaneously. Their method correlated monthly SST changes to anomalous occurrence of north and south monthly components of wind in the belt of mean westerlies, whereby the cooling of the ocean by northerly, and warming by southerly wind components clearly shows up.

Based on the long time-series of annual atmospheric surface pressure in the Icelandic area given by J. Bjerknes (1962; p. 122), spectral analysis shows that the distinctive feature of the atmospheric input to the ocean caused by the fluctuations of the Icelandic low is white noise (Moene, 1981; p. 20). This is in accordance with the spectral analysis of North Pacific data by Davis (1976; p. 249).

Uniform distribution of variance as a function of frequency, i.e. white noise, implies a lack of memory of prior states. A red spectrum in which the variance increases with decreasing frequency implies that some portion of the atmosphere–ocean–cryosphere retains a memory of prior states undoubtedly through thermal lag.

The observed perturbations of annual SST are small oscillations about a stable state of equilibrium obviously determined by the heat balance. The behavior of systems characterized by small oscillations about a stable state of equilibrium can be described by linear integro-differential equations with constant coefficients. The first approximation to a linear system is given by the first-order autoregressive linear process given by Jenkins and Watts (1968; p. 162) as

$$T\frac{\partial y}{\partial t} + y = Z(t), \tag{1}$$

where $Z(t)$ is the white noise input and T the time constant of the responding part of the system. We introduce y as the annual SST anomaly and let T represent the thermal time constant of the ocean caused by the great heat capacity. The white noise atmospheric input is represented by $Z(t)$. It appears from (1) that the feedback component of the SST changes, $\partial y/\partial t$, is proportional to $-y$; i.e., the random atmospheric input is assumed to be balanced by a negative linear oceanic feedback. The feedback of the stochastic process is described by its probability distributions.

Spectral analysis simplifies the analysis of linear systems. The power spectrum of a first-order autoregressive linear process is given by Jenkins and Watts (1968; p. 227) as

$$E_1(\omega) = \frac{A}{1 + (\omega T)^2}, \tag{2}$$

where ω is the radian frequency and A the constant white-noise spectrum of the input. In the frequency interval where

$$\omega > \frac{1}{T}, \tag{3}$$

the term $(\omega T)^2$ is the dominating one and in this inertial interval we have with high accuracy

$$E_1(\omega) = c\omega^{-2}. \tag{4}$$

According to (4) the maximum spectral power of the thermal response of the ocean to the random atmospheric input has to be expected in the low frequency region due to the great thermal time constant of the ocean, i.e., the great thermal inertia of the ocean. The model given by (2) corresponds to the stochastic model of climate variability introduced by Hasselmann (1976; pp. 473–84) in which a slow change of climate is the integral response of the ocean to continuous random excitation by shorter-time scale perturbations from the atmosphere.

2. Spectral analysis and model building

Long time-series of annual SST anomalies in the period 1880–1960 are given by J. Bjerknes (1962; p. 122) for selected test fields centered around 28°W in the North Atlantic. These time series are prolonged up to 1982 with data from weather ships and buoys. For the field centered near 53°N and covering almost 10 longitude and 5 latitude degrees, the cumulative sum of deviations of the annual SST from the mean is given in Fig. 1.

A computer program calculating the autocovariance and the power spectrum estimates of series is applied. The computational technique is appropriate for relatively short time series (Jenkins and Watts, 1968; pp. 310–312, AUTOSPEC). The calculated power spectrum estimates of the SST series are given in Fig. 2. Also shown in Fig. 2, by the broken curve, is the inertia spectrum represented by $c\omega^{-2}$. It is seen that the SST spectrum reflects the main shape of the theoretical inertia spectrum down to periods of 25–30 years, where a significant peak appears in the spectrum. A longer time series would, however, be required for a final determination of the peak.

A pronounced peak appears in a variance spectrum at the natural resonant frequency of the responding part of the system. The great thermal time constant of the ocean corresponds to a low natural resonant frequency and the observed spectral peak therefore makes sense physically. Based partly on the analysis of the available time series and mainly on physical reasons, we introduce a stochastic model given by a second-order autoregressive process.

The second-order linear process includes the possibility of a low frequency peak and is given by Jenkins and Watts (1968; pp. 37–39 and p. 164) as

$$\frac{1}{\omega_n^2}\left(\frac{\partial^2 y}{\partial t^2}\right) + \frac{2a}{\omega_n}\left(\frac{\partial y}{\partial t}\right) + y = Z(t). \tag{5}$$

Here y is the SST anomaly, $2a$ a damping factor and ω_n the natural frequency (radian) of the responding part of the system; ω_n is determined by the great heat capacity of the ocean. The spectrum is given by Jenkins and Watts (1968; p. 228) as

$$E_2(\omega) = \frac{A}{(1 - \omega^2/\omega_n^2)^2 + (2a\omega/\omega_n)^2}. \tag{6}$$

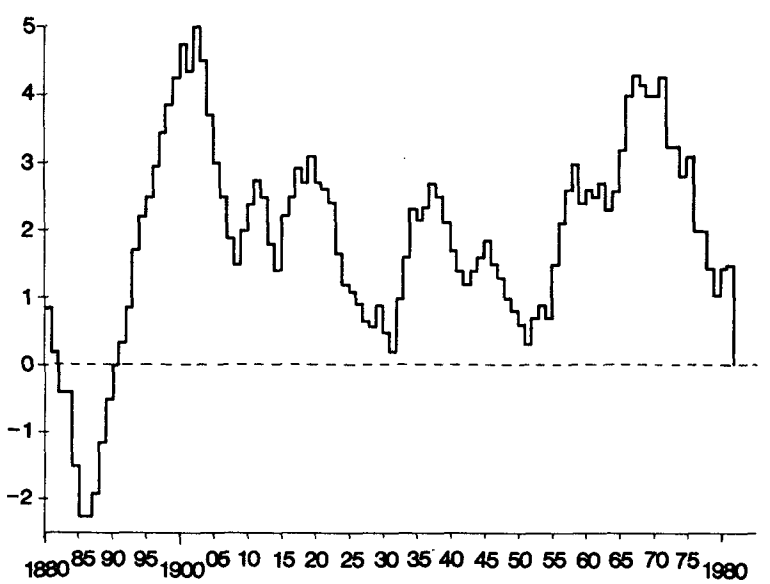

FIG. 1. The cumulative sum of deviations of the annual SST (°C) from the mean. The SST is observed in a field centered at 53°N and 28°W and covering almost 10 long and 5 lat deg.

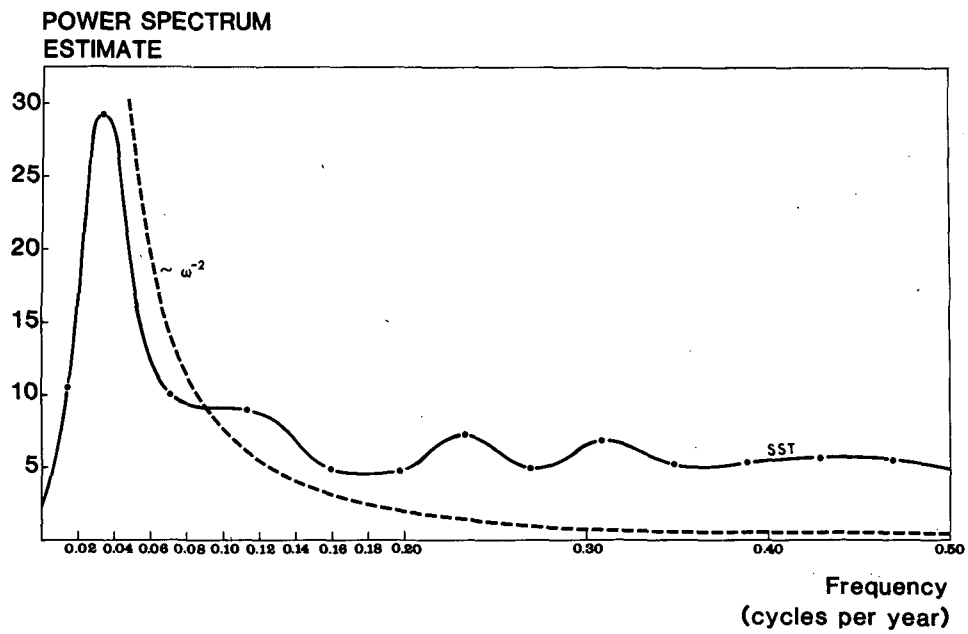

FIG. 2. The power spectrum estimates of the SST series given in Fig. 1. The broken curve is the inertia spectrum given by $c\omega^{-2}$.

The process given by (5) may be regarded as output from a second-order linear system when the input is a continuous sequence of random impulses from the atmosphere. The output from a second-order linear process is therefore a continuous disturbed periodic function. The period and phases are to some extent changing constantly due to the influence of the continuous random input $Z(t)$. Figure 1 confirms this oscillatory nature of the time series of the SST anomaly. Choosing the natural resonant frequency $f_n = 0.04$, $a = 0.3$ and $A = 10$ in (6), we obtain a theoretical inertia spectrum that also includes the observed significant low frequency peak in the SST spectrum given in Fig. 2. The process given by (5) implies the existence of a spectral peak near the natural resonant frequency determined by the inertia of the responding part of the system. The peak given by (6) is found on a slightly lower frequency than a given f_n, i.e., $f = f_n(1 - 2a^2)^{1/2}$, due to the influence of the damping term given by the damping factor $2a$ in (5). According to this model the ocean is regarded as a damped resonator. The low frequency spectral peak shown in Fig. 2 corresponds to a mean period of 25–30 years. Such a low frequency response of the ocean indicates that huge water masses must be involved through large-scale interhemispheric circulation of the ocean, including deep-water countercurrents.

3. The latitudinal oscillation of the annual mean polar frontal zone

The westerlies, appearing in annual mean surface pressure charts, are in the mean zone of the polar frontal migrating cyclones; consequently, northward or southward shifts of the belt of westerlies correspond generally to similar shifts of the annual mean polar frontal zone. The nature of the latitudinal oscillations of the annual polar frontal zone from the northeast Atlantic to northwest Europe is examined for a long period of years. It is found that the oscillations take place between two characteristic locations. The first is a southern location over northwest Europe, approximately between 50 and 60°N. The second is a northern one approximately between 60 and 70°N. Based on the annual mean surface pressure charts by Deutscher Wetterdienst (1949–82, annual issues), the years with significant northern and southern locations over northwest Europe are selected. The years with a significant northern location are found to be 1982, 1976, 1975, 1973, 1972, 1971 and 1959. Southern locations are found in the years 1981, 1980, 1967, 1966, 1965, 1962, 1960, 1958, 1957 and 1955. Comparison with Fig. 1 shows that the northern location is found in periods with dominating negative SST anomalies, and southern locations in periods with positive SST anomalies in the given area. The mean surface pressure of the years with an observed southern location is shown in Fig. 3. The southern location of the westerlies, and consequently of the mean polar frontal zone, appears in Fig. 3. The mean SST anomalies for the actual years are also shown in Fig. 3. The SST anomalies are determined by data from weather ships and buoys. The years with typical southern location of the mean polar frontal zone are characterized by positive SST anomalies in the North Atlantic. The mean surface pressure of the years with observed northern location of the

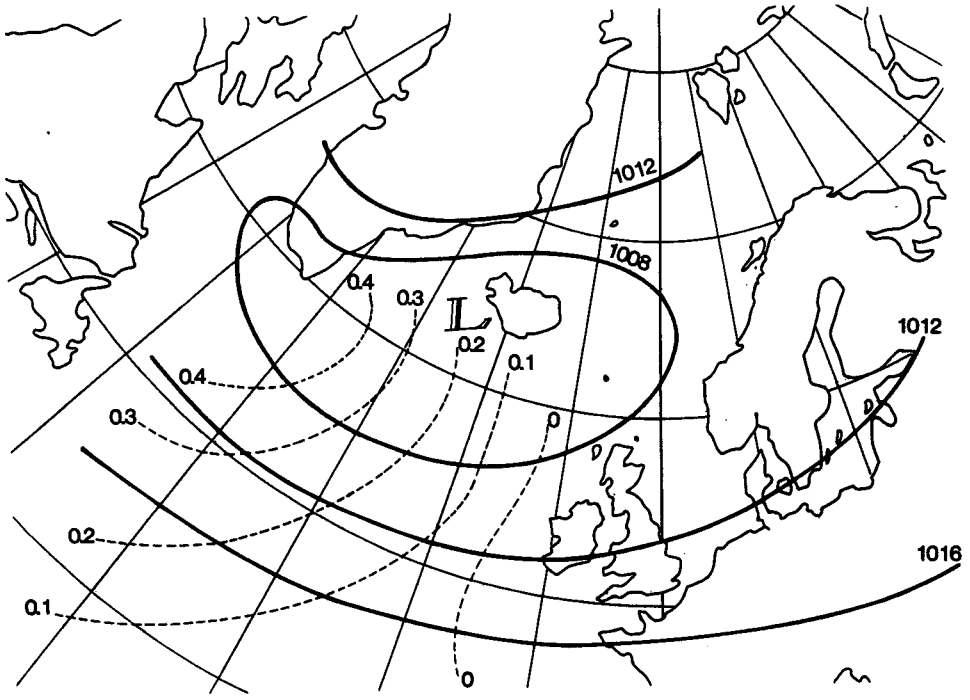

FIG. 3. The mean surface pressure of the years 1981, 1980, 1967, 1966, 1965, 1962, 1960, 1958, 1957 and 1955 with a significant southern location of the annual mean polar frontal zone (westerlies). The mean SST anomalies for the same years are given by the broken curves.

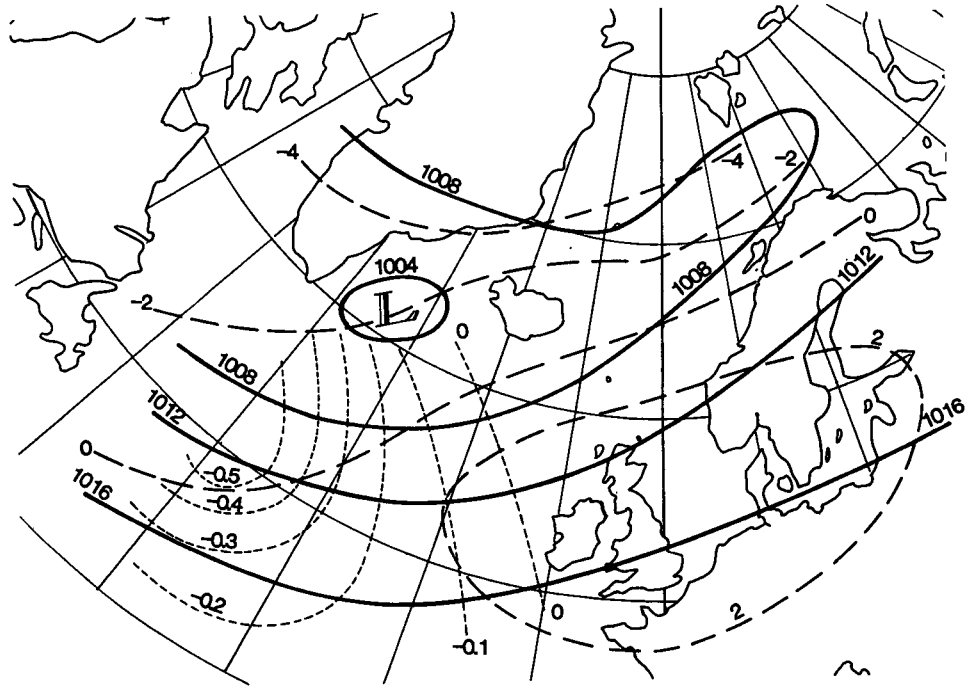

FIG. 4. The mean surface pressure of the years 1982, 1976, 1975, 1973, 1972, 1971 and 1959 with significant northern location of the annual mean polar frontal zone (westerlies). The fine broken curves represent the mean SST anomalies for the given years. The difference between the surface pressure fields of a northern and southern location of the frontal zone is given by the broken curves.

mean polar frontal zone is shown in Fig. 4. The difference between the mean surface pressure of typical northern and southern location of the westerlies is also shown in Fig. 4. The mean SST anomalies given in Fig. 4 demonstrate that the northern location of the mean polar frontal zone is associated with negative SST anomalies in the North Atlantic.

4. Low frequency oceanic thermal feedback to the atmosphere

The thermal response of the ocean to the random atmospheric input can be regarded as a second-order autoregressive linear process with a low frequency spectral peak determined by the large thermal inertia of the ocean. The years with a northern location of the annual polar frontal zone are found in periods with high probability of negative SST anomalies in the North Atlantic. The years with a southern location appear in periods with high probability of positive anomalies. The difference between the mean SST for the years with respectively northern and southern locations of the frontal zone is shown in Fig. 5. Based on the annual mean 1000–500 mb thickness, as given by Deutscher Wetterdienst (1949–82), the mean thickness of the years with a northern location of the polar frontal zone was computed. The difference between this mean thickness field and the corresponding thickness field of the years with southern location is also given in Fig. 5. The spatial correlation between the two difference fields of SST and thickness, respectively, shown in Fig. 5 is highly significant ($r = 0.92$). Periods with dominating negative SST anomalies in the North Atlantic imply atmospheric thermal fields orientated in a northeasterly direction toward Europe. In periods with dominating positive SST anomalies the orientation of the atmospheric thermal field is changed to an easterly direction toward Europe resulting in a southern location of the mean polar frontal zone. This latitudinal oscillation of the mean frontal zone can be explained by a low-frequency oceanic thermal feedback to the atmosphere.

It is of interest to observe that the area of maximum SST anomaly changes as given in Fig. 5 coincides with an important downwelling area. This area receives warm, saline watermasses of the Irminger Current, to an environment of cold, much less salty (i.e., much less dense) masses to the east from the Greenland and Labrador currents. The intense sea–air heat loss and evaporation further increases the density, both through chilling and salinity increase of the surface waters. The excess of dense surface waters must sink and feed a southward outflow of deep water estimated by Smith et al. (1937) as having an annual average of 1.9 million m^3 sec^{-1}. It may be postulated that the low frequency response of the ocean could be explained by continuous random atmospheric disturbances of the surface part of an interhemispheric circulation system of the ocean.

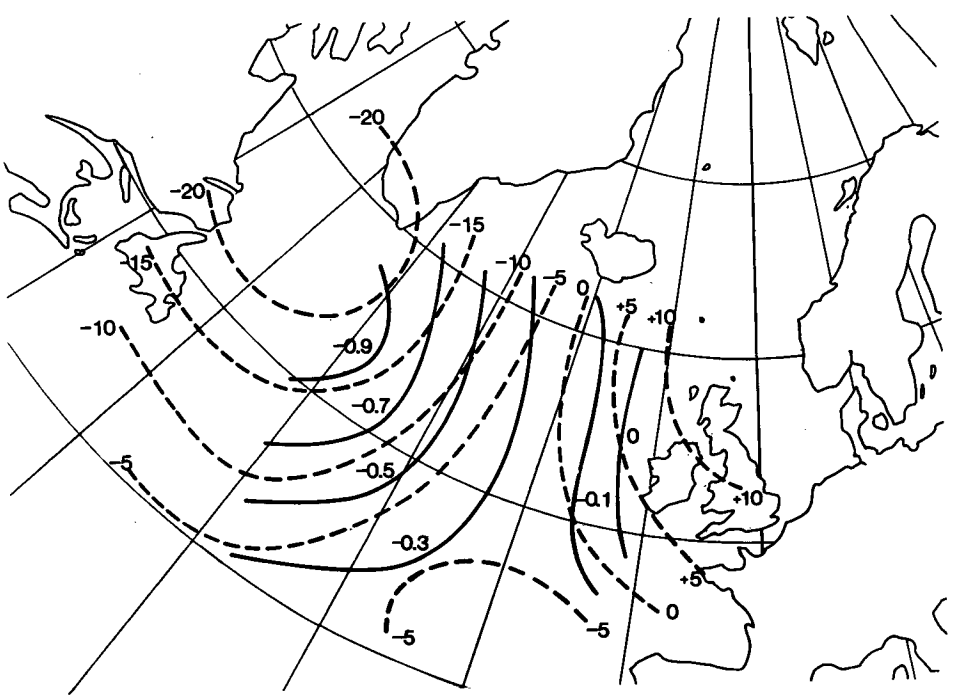

FIG. 5. The difference between the mean SST of the years with a northern and southern location of the annual polar frontal zone. The broken curves represent the difference (gpm) between the mean 1000–500 mb thickness of the corresponding two periods of years.

5. Results of the latitudinal oscillation of the annual polar frontal zone over northwest Europe

The mean large-scale distribution of precipitation for the given years with a significant southern location of the annual frontal zone is shown in Fig. 6. The mean distribution for the years with a significant northern location of the frontal zone is also shown in Fig. 6 (right). The given large-scale distributions of annual precipitation anomalies are computed from the annual large-scale anomalies published by Deutscher Wetterdienst (1949–82). Figure 6 shows that the mean anomalies of the years with a southern location of the frontal zone are characterized by above normal precipitation from central west Europe toward the east and northeast. An area of below normal precipitation appears in central and northern Norway. This period of years, including most of the 1960s, is characterized by frequent floods in central west Europe. The mean precipitation anomalies of the years with a significant northern location of the polar frontal zone are characterized by below normal precipitation from central west Europe toward the east and northeast. This period, including most of the 1970s, is characterized by several severe droughts in central west Europe. Above normal precipitation is found in central and northern Norway. The large gradient along the north–south orientated mountain chain in Norway and Sweden is remarkable in both of the typical situations. This gradient is explained by the latitudinal oscillation of the westerlies. In the case of a northern location of the westerlies, the west wind components transporting maritime airmasses toward the mountain chain result in a precipitation maximum in the catchment area formed by the western slope of the mountains. On the east side of the mountain chain, dry conditions prevail due to subsidence. In the case of a southern location of the polar frontal zone, the westerlies over Scandinavia are weakened and replaced by more frequent easterly wind components, resulting in above normal precipitation on the eastern side of the mountain chain and below normal precipitation on the western side. It is shown in an earlier work (Moene, 1981) that these distinctive features are also reflected in the runoff of two rivers, one in central Norway, Namsen, located about 65°N; and one in southeast Norway, Glomma, located between 59° and 63°N. The precipitation catchment area of the river Namsen in central Norway is formed by the western slope of the mountains and has maximum precipitation in the case of a northern location of the polar frontal zone. The river Glomma in southeast Norway has a precipitation catchment area formed mainly by the east and southeast slope of the mountains and the maximum precipitation occurs with a southern location of the polar frontal zone. Figure 7 shows the cumulative sum of annual runoff anomalies for the two rivers. It appears that for periods of 25–30 years the general long-term trends of the cumulative runoffs

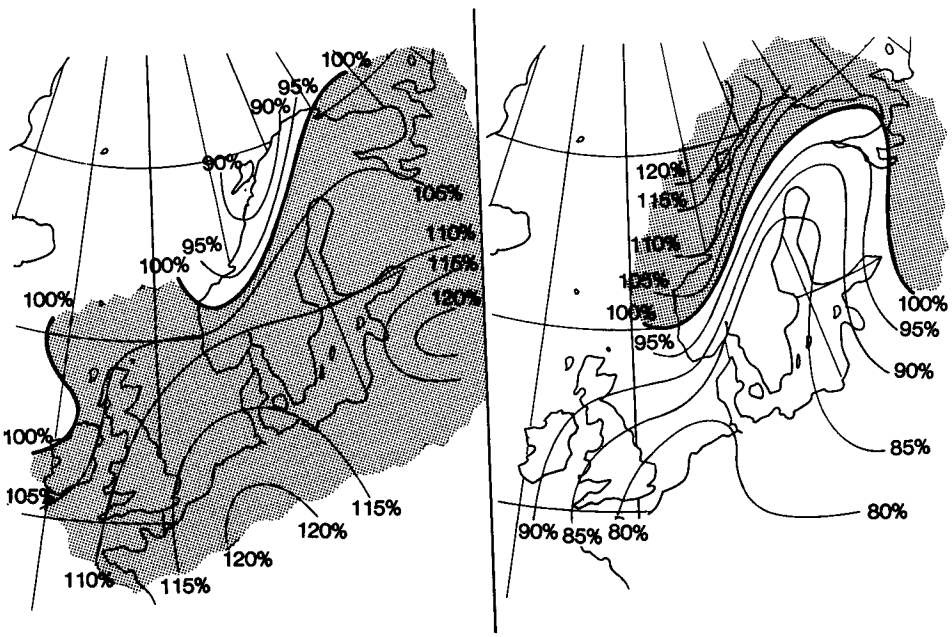

FIG. 6. The mean large-scale distribution of precipitation (percent of normal) of the years 1981, 1980, 1967, 1966, 1965, 1962, 1960, 1958, 1957 and 1955 with a southern location of the annual polar frontal zone (left), and the years 1982, 1976, 1975, 1973, 1972, 1971 and 1959 with a northern location of the frontal zone (right).

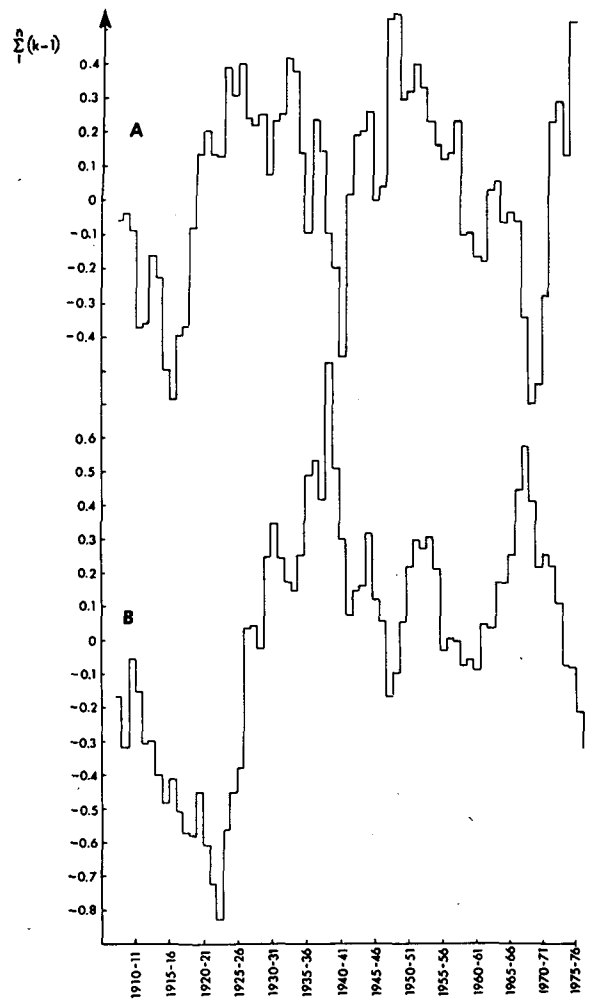

FIG. 7. The cumulative sum of deviations $\sum_1^n (k - 1)$, where $k = r/r_{mean}$ and r is annual runoff. Part A is the sum for the river Namsen located in central Norway (about 65°N) with a precipitation maximum in the case of a northern location of the annual polar frontal zone. Part B is the sum for the river Glomma located in southeast Norway (between 59° and 63°N) with a precipitation maximum in the case of a southern location of the annual polar frontal zone.

from the two catchment areas are inverse. Spectral analysis of the runoff time series shows that the broad features of the runoff spectra are given by the SST spectrum in Fig. 2, i.e., significant low-frequency peaks coincide at a frequency corresponding to a period length of 25–30 years (Moene, 1981; p. 18). This is an indication of the relationship between the low-frequency oscillation of the SST in the given area in the North Atlantic and the latitude oscillation of the annual polar frontal zone. The final verification of these associations depends on longer time series than the present series.

6. Conclusions

Analysis of the available North Atlantic SST time series indicates that the interaction of sea and atmosphere can be regarded as an autoregressive linear stochastic process of second order with white noise atmospheric input. The low-frequency peak of the SST spectrum can be explained physically by a very low natural frequency caused by the great thermal inertia of the responding ocean. The spectral peak found at a frequency corresponding to a period between 20 and 30 years indicates that huge water-masses must be involved in the process. A longer time series is required for a final verification of the peak.

The response of a second-order autoregressive linear system to a random input of continuous impulses is a disturbed periodic oscillation. This nature of the oscillation is confirmed by the available SST time series.

The probable oceanic low-frequency thermal feedback to the atmosphere is examined in those years 1950–82, for which upper air data are available. The period 1950–82 is also of particular interest because it includes a marked period of low-frequency SST oscillation. A southern location of the annual polar frontal zone is frequent in the first half of the period, which is dominated by positive SST anomalies in the central North Atlantic. A northern location of the polar frontal zone over northwest Europe is frequent in the second half of the period, which is dominated by negative SST anomalies. The changes in the mean SST in the North Atlantic for the given significant years of the first half of the period compared to the mean SST of the significant years of the second half of the period are highly positively correlated with the corresponding 1000–500 mb thickness changes of the overlying atmosphere. This indicates a low-frequency thermal feedback from the ocean to the atmosphere explaining the observed low-frequency latitudinal oscillation of the annual polar frontal zone over northwest Europe.

The result of the latitudinal oscillation of the annual polar frontal zone is demonstrated by the mean large-scale precipitation anomalies of the years with either a northern or southern location of the frontal zone over west Europe. In the 1970s, with significant northern location, frequent severe droughts occurred in central west Europe. In the 1960s, with a significant southern location, severe floods occurred frequently in central west Europe. A large precipitation anomaly gradient appears across the north–south oriented mountain chain in the Scandinavian peninsula. A low-frequency oscillation with opposite phase is observed in the long time-series of the runoff of two rivers in Norway, located on the western and eastern side of the mountain chain. The broad features of the runoff spectra are similar to the North Atlantic SST spectrum with a significant spectral peak located at the same low fre-

quency. This is another indication of a low frequency thermal feedback from the ocean to the atmosphere.

Acknowledgments. The comments, particularly of one anonymous reviewer, have been most helpful in preparing this article.

REFERENCES

Bjerknes, J., 1962: Synoptic survey of the interaction of sea and atmosphere in the North Atlantic. *Geophys. Norv.*, **24**(3), 115–145.

Davis, R. E., 1976: Predictability of sea surface temperature and sea level pressure anomalies over the North Pacific ocean. *J. Phys. Oceanogr.*, **6**, 246–266.

Deutscher Wetterdienst, 1949–1978: *Die Grosswetterlagen Europas.* Offenbach, Annual issues.

Hasselmann, K., 1976: Stochastic climate models. Part 1. Theory. *Tellus*, **28**, 473–484.

Helland-Hansen, B., and F. Nansen, 1917: Temperaturschwankungen des Nordatlantischen Ozeans und in der Atmosphere. *Videnskapsselskapets Skrifter*, I. Mat.-Naturv. Klasse 1916, **9**, University Press, Oslo.

Jenkins, G. M., and D. Watts, 1968: *Spectral Analysis and Its Applications.* Holder-Day, 1–320.

Moene, A., 1981: On the latitudinal oscillations of the northeast Atlantic annual mean polar frontal zone. *Geophys. Norv.*, **32**(2), 15–21.

Smith, E. H., F. M. Soule and O. Mosby, 1937: The Marion and General Green expeditions to Davis Strait and Labrador Sea 1928–31–33–34–35. *U.S. Coast Guard Bull. Phys. Oceanogr.*, **19**.